Polymer Journal (2012) 44, 907–912

www.nature.com/pj

ORIGINAL ARTICLE

Field-dependent ^{19}F NMR study of sperm whale myoglobin reconstituted with a ring-fluorinated heme

Yasuhiko Yamamoto[1], Satoshi Nagao[1,3], Yueki Hirai[1], Hulin Tai[1] and Akihiro Suzuki[2]

A synthetic heme possessing immobilized fluorine atoms as peripheral side chains has been incorporated into the apoprotein of sperm whale myoglobin (Mb), and the field dependence of the line width of ^{19}F NMR signals observed for the protein with *S* values ranging from 0 to 5/2 was analyzed in order to gain a quantitative insight into the ^{19}F transverse relaxation mechanism in Mb with various magnetic properties. In the cases of deoxy ($S=2$) and met-aquo ($S=5/2$) Mbs, the significant contribution of Curie spin relaxation to the ^{19}F transverse relaxation was demonstrated and analysis of the Curie spin relaxation was useful to estimate the overall correlation time of the protein.
Polymer Journal (2012) **44,** 907–912; doi:10.1038/pj.2012.60; published online 18 April 2012

Keywords: Curie spin relaxation; ^{19}F NMR; myoglobin; paramagnetic relaxation; paramagnetic shift

INTRODUCTION

The analysis of nuclear relaxation has provided a wealth of information about structural and dynamic properties of molecules. In particular, in the case of metalloproteins carrying unpaired electron(s), the dynamic nature of a molecule is sharply manifested in paramagnetic relaxation observed on paramagnetically shifted nuclear magnetic resonance (NMR) signals.[1–4] In the present study, we have analyzed the field dependence of the line widths of NMR signals of sperm whale myoglobins (Mbs) with a variety of magnetic properties in order to elucidate field-dependent properties of the paramagnetic relaxation. Mb is an oxygen-binding hemoprotein with a molecular weight of ~17 kDa (Figure 1a), and a single heme (Figure 1b) is embedded in its protein matrix. The side chain of a His residue is coordinated to the heme iron as an axial ligand, and an exogenous ligand, such as not only the dioxygen molecule (O_2), but also a carbon monoxide (CO) or water molecule (H_2O), and cyanide ion (CN^-) is bound to the iron on the side of the heme opposite the axial His (Figure 1d). The heme iron in Mb is either in the ferrous or ferric state, and hence, depending upon the degree of spin pairing of electrons in the 3*d* orbitals, ferrous heme iron can have 4, 2 or 0 unpaired electrons, corresponding to total spin quantum number $S=2$, 1 or 0, respectively, and for ferric heme iron $S=5/2$, 3/2 or 1/2 with 5, 3 or 1 unpaired electron, respectively. The spin state of Mb depends on the chemical nature of the exogenous ligand. For ferrous heme iron, the deoxy (no ligand) form (deoxyMb) is penta-coordinated with a high-spin configuration, $S=2$, and the oxy (MbO_2) or carbonmonoxy form (MbCO) possesses a low-spin configuration, $S=0$ (Figure 2). On the other hand, the coordination of H_2O to ferric heme iron gives high-spin state $S=5/2$ (metMb), low-spin state $S=1/2$ being obtained with CN^- ($MbCN^-$) (Figure 2).

By virtue of the absence of interfering background signals, the introduction of fluorine atom(s) into the peripheral side chain(s) of the heme facilitates the observation of their signals in various oxidation, spin and ligation states of the protein.[5–11] ^{19}F is a 100% abundant nucleus with nuclear spin $I=1/2$ and, because of a relatively high gyromagnetic ratio, ^{19}F NMR is ~83% as sensitive as ^{1}H NMR. In addition, because of the wider spectral range for ^{19}F NMR than ^{1}H NMR, individual signals will be better resolved on ^{19}F NMR.[12,13] A ring-fluorinated heme, 13,17-bis(2-carboxylatoethyl)-3,7-difluoro-2,8,12,18-tetramethyl-porphyrinatoiron(III) (3,7-DF (Figure 1c)),[5] has been incorporated into Mb, and the field dependence of ^{19}F NMR signals arising from MbCO ($S=0$), $MbCN^-$ ($S=1/2$), deoxyMb ($S=2$) and metMb ($S=5/2$) has been analyzed in order to evaluate the ^{19}F relaxation mechanism in the proteins. Despite considerably large line widths of paramagnetically shifted signals, the high sensitivity and excellent signal resolution of ^{19}F NMR allowed the observation of well-separated signals in the spectra of all the paramagnetic Mbs examined in the study. Furthermore, as the fluorine atoms introduced to the heme as peripheral side chains are dynamically fixed to the porphyrin ring, detailed analysis of the field dependence of the line widths of the ^{19}F signals was useful to estimate the correlation time (τ_r) of the heme accommodated in the active site of the protein.

[1]Department of Chemistry, University of Tsukuba, Tsukuba, Japan and [2]Department of Materials Engineering, Nagaoka National College of Technology, Nagaoka, Niigata, Japan
[3]Current address: Graduate School of Materials Science, Nara Institute of Science and Technology, Nara 630-0192, Japan.
Correspondence: Professor Y Yamamoto, Department of Chemistry, University of Tsukuba, Tsukuba 305-8571, Japan.
E-mail: yamamoto@chem.tsukuba.ac.jp
Received 16 January 2012; revised 22 February 2012; accepted 6 March 2012; published online 18 April 2012

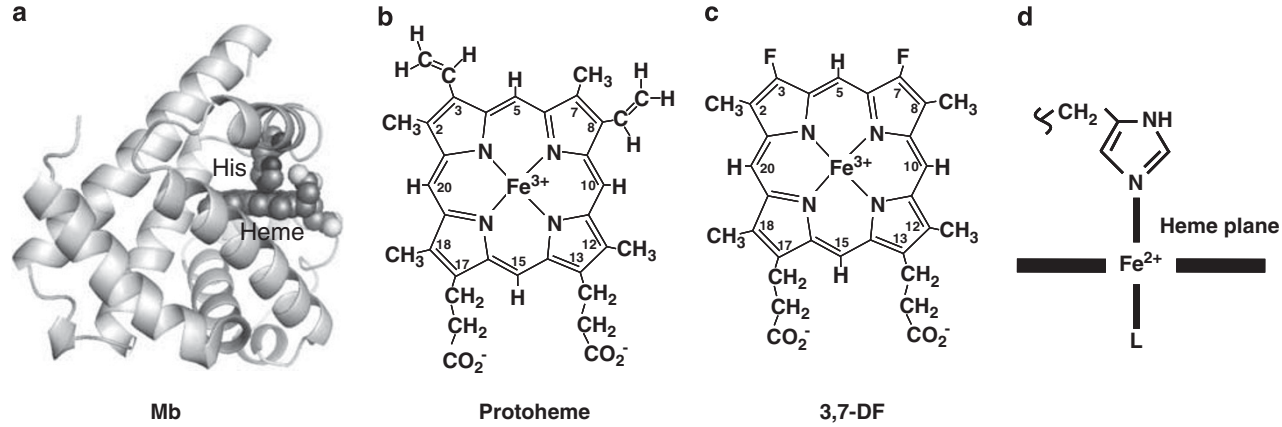

Figure 1 Schematic representation of the structure of Mb (**a**), molecular structures of heme (**b**) and 3,17-bis(2-carboxyethyl)-3,7-difluoro-2,8,12,18-tetramethylporphyrinatoiron(III) (3,7-DF) (**c**), and heme coordination structure (**d**). L in **d** represents an exogenous ligand.

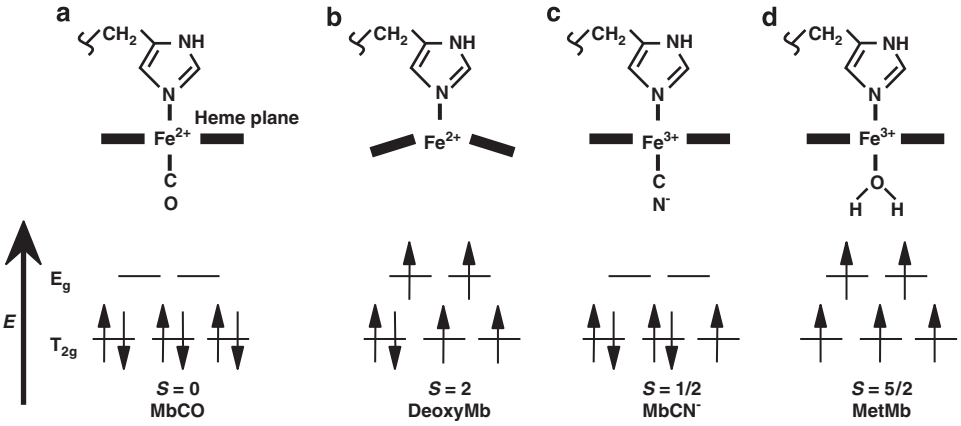

Figure 2 Heme coordination structures and 3*d* electron configulations in MbCO (**a**), deoxyMb (**b**), $MbCN^-$ (**c**) and metMb (**d**).

The nuclear relaxation rate (R_{obs}) in a paramagnetic system is expressed as the sum of diamagnetic (R_{dia}) and paramagnetic (R_{para}) terms,[1]

$$R_{obs} = R_{dia} + R_{para}. \quad (1)$$

R_{dia} is written as the sum of the contributions of the dipole–dipole interaction (R_{dia}^{DD}), chemical shift anisotropy (R_{dia}^{CSA}), and others (R_{dia}^{other}),

$$R_{dia} = R_{dia}^{DD} + R_{dia}^{CSA} + R_{dia}^{other}. \quad (2)$$

The contributions of R_{dia}^{CSA} to the nuclear spin–lattice (R_{1dia}) and spin–spin (R_{2dia}) relaxation rates (R_{1dia}^{CSA} and R_{2dia}^{CSA}, respectively) depend on the magnetic field strength and can be written as follows,[14]

$$R_{1dia}^{CSA} = \frac{6}{40}\omega_I^2\delta_z^2(1+\frac{\eta^2}{3})J(\omega_I) \quad (3)$$

$$R_{2dia}^{CSA} = \frac{1}{40}\omega_I^2\delta_z^2(1+\frac{\eta^2}{3})(3J(\omega_I)+4J(0)) \quad (4)$$

$$J(\omega_I) = \frac{2\tau_r}{1+\omega_I^2\tau_r^2}, \quad (5)$$

where $\delta_z$is associated with the principal components of the chemical shift tensor, η is the asymmetric parameter of the molecule under consideration, and $J(\omega_I)$ represents the spectral density function.

On the other hand, R_{para} is expressed as the sum of the contributions of metal-centered (R_{para}^{MC}) and ligand-centered (R_{para}^{LC}) dipolar terms, the contact hyperfine interaction (R_{para}^{C}), and Curie spin relaxation (R_{para}^{Curie}),[1]

$$R_{para} = R_{para}^{MC} + R_{para}^{LC} + R_{para}^{C} + R_{para}^{Curie}. \quad (6)$$

Using the Solomon–Bloembergen equations,[15,16] together with the expression of R_{para}^{Curie},[17,18] paramagnetic contributions to the nuclear spin–lattice and spin–spin relaxation rates (R_{1para} and R_{2para}, respectively) in a paramagnetic system are expressed by

$$\begin{aligned} R_{1para} = {} & \frac{2}{15}(\frac{\mu_0}{4\pi})^2\gamma_I^2\beta_e^2\mu_B^2S(S+1)(\gamma_M^{-6}+\Sigma\rho^2\gamma_L^{-6}) \\ & \times\left[\frac{\tau_{c2}}{1+(\omega_I-\omega_S)^2\tau_{c2}^2}+\frac{3\tau_{c1}}{1+\omega_I^2\tau_{c1}^2}+\frac{6\tau_{c2}}{1+(\omega_I+\omega_S)^2\tau_{c2}^2}\right] \\ & +\frac{2}{3}S(S+1)(\frac{A}{\hbar})^2\left[\frac{\tau_{e2}}{1+(\omega_I+\omega_S)^2\tau_{e2}^2}\right] \\ & +\frac{2}{5}(\frac{\mu_0}{4\pi})^2\frac{\omega_I^2\beta_e^4\mu_B^4S^2(S+1)^2}{(3kT)^2r_M^6}(\frac{3\tau_r}{1+\omega_I^2\tau_r^2}) \end{aligned} \quad (7)$$

$$R_{2\mathrm{para}} = \frac{1}{15}\left(\frac{\mu_0}{4\pi}\right)^2\gamma_I^2\beta_e^2\mu_B^2 S(S+1)\left(\gamma_M^{-6}+\Sigma\rho^2\gamma_L^{-6}\right)$$
$$\times\left[4\tau_{c1}+\frac{3\tau_{c2}}{1+(\omega_I-\omega_S)^2\tau_{c2}^2}+\frac{3\tau_{c1}}{1+\omega_I^2\tau_{c1}^2}\right.$$
$$\left.+\frac{6\tau_{c2}}{1+\omega_S^2\tau_{c2}^2}+\frac{6\tau_{c2}}{1+(\omega_I+\omega_S)^2\tau_{c2}^2}\right] \quad (8)$$
$$+\frac{1}{3}S(S+1)\left(\frac{A}{\hbar}\right)^2\left[\tau_{e1}+\frac{\tau_{e2}}{1+(\omega_I-\omega_S)^2\tau_{e2}^2}\right]$$
$$+\frac{1}{5}\left(\frac{\mu_0}{4\pi}\right)^2\frac{\omega_I^2\beta_e^4\mu_B^4S^2(S+1)^2}{(3kT)^2r_M^6}\left(4\tau_{c2}+\frac{3\tau_r}{1+\omega_I^2\tau_r^2}\right)$$

$$\tau_{c1}^{-1} = T_{1e}^{-1}+\tau_r^{-1}+\tau_{ex}^{-1} \quad (9)$$

$$\tau_{c2}^{-1} = T_{2e}^{-1}+\tau_r^{-1}+\tau_{ex}^{-1} \quad (10)$$

$$\tau_{e1}^{-1} = T_{1e}^{-1}+\tau_{ex}^{-1} \quad (11)$$

$$\tau_{e2}^{-1} = T_{2e}^{-1}+\tau_{ex}^{-1}, \quad (12)$$

where, in the present case, r_M and r_L are the distance between the F and Fe atoms, and the F–C bond length, respectively, ρ is the unpaired electron density at the carbon and fluorine atoms at positions 3 and 7 on the porphyrin of 3,7-DF (Figure 1c), $(\frac{A}{\hbar})$ is the apparent hyperfine coupling constant for ^{19}F, ω_I and ω_S are the Larmor frequencies of ^{19}F and electron, respectively, T_{1e} and T_{2e} are the electron longitudinal and transverse relaxation times, respectively, and τ_{ex} is the electron exchange time. The other parameters are as usual. In large molecules with highly resolved NMR spectra, $T_{1e}, T_{2e} << \tau_r$ and at high magnetic field, $\omega_I^2T_{1e}^2 << 1$, $1 < \omega_S^2T_{1e}^2$, and $1 < \omega_S^2T_{2e}^2$, Equations (7) and (8) are reduced to the equations[19,20]

$$R_{1\mathrm{para}} = \frac{2}{15}\left(\frac{\mu_0}{4\pi}\right)^2\gamma_I^2\beta_e^2\mu_B^2S(S+1)\left(\gamma_M^{-6}+\Sigma\rho^2\gamma_L^{-6}\right)T_{1e} \quad (13)$$

$$R_{2\mathrm{para}} = \frac{7}{15}\left(\frac{\mu_0}{4\pi}\right)^2\gamma_I^2\beta_e^2\mu_B^2S(S+1)\left(\gamma_M^{-6}+\Sigma\rho^2\gamma_L^{-6}\right)T_{1e}$$
$$+\frac{1}{3}S(S+1)\left(\frac{A}{\hbar}\right)^2T_{1e}+\frac{4}{5}\left(\frac{\mu_0}{4\pi}\right)^2\frac{\omega_I^2\beta_e^4\mu_B^4S^2(S+1)^2}{(3kT)^2r_M^6}\tau_r. \quad (14)$$

Equation (14) dictates that $R_{2\mathrm{para}}$ depends on the field strength owing to the contribution of $R_{2\mathrm{para}}^{\mathrm{Curie}}$, the third term on the right-hand side of the equation. The nuclear spin–lattice ($R_1 = R_{1\mathrm{dia}} + R_{1\mathrm{para}}$) and spin–spin ($R_2 = R_{2\mathrm{dia}} + R_{2\mathrm{para}}$) relaxation rates of a paramagnetic Mb are schematically plotted against the square of the applied field strength, ω_I^2 (Figure 3a), and a significant effect of $R_{2\mathrm{para}}^{\mathrm{Curie}}$ on R_2 is demonstrated in the plots. In this study, analysis of the field dependence of the line widths of the signals allowed us to estimate $R_{2\mathrm{para}}^{\mathrm{Curie}}$, which can be interpreted quantitatively in terms of the τ_r value.

EXPERIMENTAL PROCEDURES

Sample preparation

Mb was purchased as a lyophilized powder from Biozyme and used without further purification. The apoprotein of Mb was prepared at 4 °C according to the procedure of Teale.[21] 3,7-DF chloride was synthesized as previously described.[5] Reconstitution of the apoprotein with heme was carried out by the standard procedure.[5,6] The reconstituted Mb was concentrated to ~1 mM in an ultrafiltration cell (Amicon, Merck Millipore, Billerica, MA, USA) and the solvent was exchanged with 90% H_2O/10%^2H_2O. A 10-fold molar excess of potassium cyanide was added to metMb to prepare $MbCN^-$. MbCO was prepared by the injection of CO gas (Japan Air Gases) and the addition of $Na_2S_2O_4$ (Wako Pure Chemical Industries, Ltd., Osaka, Japan). DeoxyMb was prepared from metMb, which had been evacuated and flushed with N_2 gas (Japan air gases) several times, by the addition of $Na_2S_2O_4$. The pH of the sample is the direct read of a pH meter (Horiba F-22 equipped with a Horiba type 6069-10c electrode). The p^{2}H of the sample was adjusted using 0.2 M NaO^2H or ^2HCl.

^{19}F NMR measurements

^{19}F NMR spectra were recorded on either a Bruker AC-400 P or AVANCE-500 FT-NMR spectrometer operating at a ^{19}F frequency of 376 ($B_0 = 9.4$ T) or 471 ($B_0 = 11.7$ T) MHz, respectively. A typical spectrum consisted of 20 k transients with a 100 kHz spectral width and 8 k data points. The signal-to-noise ratio of the spectrum was improved by apodization, which introduced 20–100 Hz line broadening. The NMR spectra were processed using XWIN-NMR version 3.5 (Bruker BioSpin, Karlsruhe, Germany) and line-shape analysis of the signals was performed using MestRe-c version 4.8.6.0 (Mestrelab Research) to obtain their line widths ($\Delta\nu_{1/2}^{\mathrm{obs}}$). Chemical shifts are given in p.p.m. downfield from trifluoroacetic acid as an external reference.

RESULTS AND DISCUSSION

The 376 MHz ^{19}F NMR spectra of various forms of Mb reconstituted with 3,7-DF are illustrated in Figure 4. The signal assignments were obtained on the basis of ^{19}F–^{1}H nuclear Overhauser effect

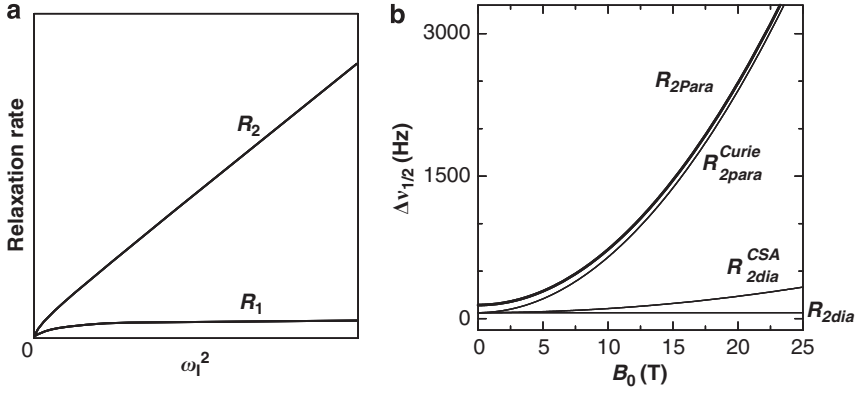

Figure 3 Plots of nuclear spin–lattice (R_1) and spin–spin (R_2) relaxation rates against the square of the magnetic field strength (ω_I^2) for a system with $\omega_I^2\tau_r^2 >> 1$ (**a**) and ones of the $R_{2\mathrm{dia}}$, $R_{2\mathrm{dia}}^{\mathrm{CSA}}$, and $R_{2\mathrm{para}}^{\mathrm{Curie}}$ contributions to the line width ($\Delta\nu_{1/2}$) against the magnetic field strength (B_0) for deoxyMb with $S = 2$ (B). In (**b**), the $R_{2\mathrm{dia}}$ and $R_{2\mathrm{dia}}^{\mathrm{CSA}}$ contributions were calculated from the results for MbCO with $S = 0$, and $R_{2\mathrm{para}}$ is the sum of $R_{2\mathrm{dia}}$, $R_{2\mathrm{dia}}^{\mathrm{CSA}}$, and $R_{2\mathrm{para}}^{\mathrm{Curie}}$.

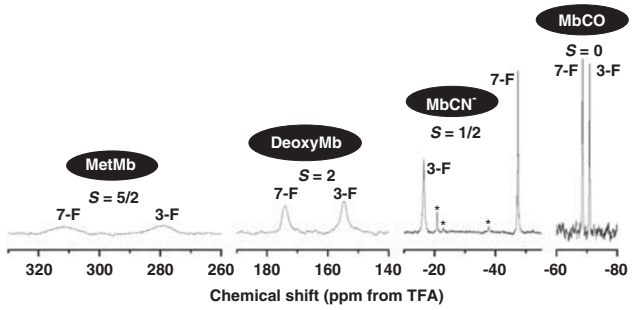

Figure 4 The 376 MHz ^{19}F NMR spectra of MbCO, MbCN$^-$, deoxyMb and metMb reconstituted with 3,7-DF in 90% H_2O/10% ^2H_2O, pH 7.0, at 25 °C. The signal assignments are indicated with the spectra. The peaks labeled with asterisks are because of impurities.

Table 1 ^{19}F chemical shifts and line widths of Mbs possessing 3,7-DF in 90% ^1H_2O/10%^2H_2O, pH 7.0, at 25 °C

				$\Delta\nu_{1/2}^{obs}$[a] *(Hz)*	
Mb	*S*	*Signal*	δ_{obs}[b] *(p.p.m.)*	$B_0 = 9.4$ *T*	$B_0 = 11.7$ *T*
MbCO	0	3-F	−71.0	81 ± 8	98 ± 10
		7-F	−68.6	107 ± 11	129 ± 13
MbCN$^-$	1/2	3-F	−16.3	203 ± 20	250 ± 25
		7-F	−47.4	120 ± 12	121 ± 12
DeoxyMb	2	3-F	159.4	710 ± 71	910 ± 91
		7-F	177.9	660 ± 66	950 ± 95
MetMb	5/2	3-F	275.8	4800 ± 480	5300 ± 530
		7-F	309.7	5600 ± 560	ND[c]

[a]Observed line width.
[b]Observed shift.
[c]Not determined because of extensive line broadening.

connectivities and spectral comparison with Mbs reconstituted with other fluorinated hemes.[5,6] As described previously,[5] the observation of two signals in the ^{19}F NMR spectrum of MbCO (Figure 4) was the result of removal of the degeneracy of the magnetic environments of the two fluorine atoms of two-fold symmetric 3,7-DF through a heme–protein interaction. The shifts of the signals were closely related to the *S* value of the protein. In the spectrum of paramagnetic MbCN$^-$ (Figure 4), the 3- and 7-F signals were downfield-shifted by 54.7 and 21.2 p.p.m., respectively, relative to the corresponding ones of MbCO, at 25 °C, and the signals of deoxyMb and metMb were downfield-shifted to > 200 and > 300 p.p.m., respectively, relative to those of MbCO. On the other hand, the separation values of the two signals of MbCO, MbCN$^-$, deoxyMb, and metMb at 25 °C were 2.4, 31.1, 18.5 and 33.9 p.p.m., respectively. The relatively large separation for the MbCN$^-$ signals is due to its large in-plane asymmetry in the heme electronic structure. Furthermore, the non-equivalence of the line widths between the 3- and 7-F signals of each Mb is predominantly due to the difference in the contribution of the contact interaction to spin–spin relaxation rate.[20]

The line widths of the signals ($\Delta\nu_{1/2}^{obs}$) ranged from ~100 Hz for MbCO with $S = 0$ to > 4000 Hz for metMb with $S = 5/2$. The considerable broadening of the signals with increasing *S* value demonstrated the significant contributions of the paramagnetic relaxation mechanisms to the R_2 value (Figure 4). The line widths of the signals at 9.4 T were compared with those of the corresponding signals at 11.7 T (Table 1). For all the signals observed, the line widths at the higher field strength were larger than those at the lower field strength. In addition, the difference in the line width between the signals recorded at two different field strengths increased with increasing *S* value, indicating the significant contributions of the R_{para}^{Curie} values to the R_2 values of the signals.

In the case of diamagnetic MbCO, the increase in the line width of the signals observed at higher magnetic field is attributed solely to the R_{2dia}^{CSA} contribution. As shown in Table 2, the differences in the R_2^{obs} values calculated from the $\Delta\nu_{1/2}^{obs}$ values (ΔR_2^{obs}) yielded the R_{2dia}^{CSA} values. In order to calculate the ΔR_2^{obs} values, $\omega_I^2\tau_r^2 >> 1$ was assumed (see below), and hence equation (4) was reduced to $R_{2dia}^{CSA} = \frac{1}{10}\omega_I^2\delta_z^2 J(0)$. The calculated ΔR_2^{obs} value for 3-F(or 7-F) is proportional to $\frac{1}{10}\delta_z^2(1+\frac{\eta^2}{3})J(0)(\omega_{I2}^2 - \omega_{I1}^2)$, where ω_{I1} and ω_{I2} are 376 and 471 MHz, respectively, and hence its R_{2dia}^{CSA} value at a given field strength could be calculated without the knowledge of the other parameters. The obtained values indicated that the R_{2dia}^{CSA} contributions to the R_2^{obs} values of the signals at 9.4 T and 11.7 T are ~35% and ~50%, respectively.

For paramagnetic MbCN$^-$ with $S = 1/2$, the line width of the 3-F signal was larger by a factor of about two compared with that of the 7-F signal. The large difference in the $\Delta\nu_{1/2}^{obs}$ value between the signals of MbCN$^-$ is predominantly attributed to the R_{2para}^{C} contribution, because the paramagnetic shift calculated using the shift of MbCO as a diamagnetic reference shift was much larger for the 3-F signal than the 7-F one, that is, 54.7 and 21.2 p.p.m. for the former and latter, respectively. The small R_{2para}^{Curie} contributions to the R_{2obs} values of the signals were clearly manifested in the relatively small field dependence of their $\Delta\nu_{1/2}^{obs}$ values.

In the case of deoxyMb with $S = 2$, the $\Delta\nu_{1/2}^{obs}$ values at 11.7 T increased by ~200 Hz relative to those of the corresponding signals at 9.4 T. The large field dependence of the $\Delta\nu_{1/2}^{obs}$ values could be accounted for by the R_{2dia}^{CSA} and R_{2para}^{Curie} contributions to the R_{2obs} values, and the close correlation between the *S* value and the magnitude of the field dependence of the $\Delta\nu_{1/2}^{obs}$ value (Table 1) indicated that the latter contribution is much larger than the former. Assuming that the R_{2dia}^{CSA} contribution is independent of the oxidation, ligation and spin state of Mb, the R_{2para}^{Curie} value of deoxyMb could be estimated using the data obtained for MbCO, as summarized in Table 3. As shown in Table 3, the R_{2para}^{Curie} value largely accounts for the R_{2para} value, which predominantly determines the R_{2obs} values of the signals of deoxyMb. Analysis of the R_{2para}^{Curie} contribution to the signals of deoxyMb, through the third term of equation (14), was useful for estimating the τ_r value of Mb. Values of ~30 ns were obtained for the τ_r value, these values being larger compared with those reported previously, that is, ~20 ns.[22–24] The τ_r value estimated on 7-F signal exhibited larger deviation from the previously reported values than that on 3-F one, and hence the magnitude of the overestimation of the τ_r value using the present method could be related to the paramagnetic shifts of the signals. The observed paramagnetic shift is the sum of both contact and pseudo-contact shifts due to delocalization of unpaired electrons and magnetic anisotropy arising from unpaired electrons at heme Fe, respectively, and the separation of the two signals of a given paramagnetic Mb is attributed largely to the difference in the contact shift between them. The contact shift of the 3-F(or 7-F) signal is determined by the unpaired electron density in the p_z (p_π) orbital of the pyrrole carbon atom to which the fluorine atom is attached, and hence the separation of the two signals is likely to reflect the non-equivalence in electronic nature between the two F–C bonds. Consequently, the larger separation of the two signals for deoxyMb than MbCO (Table 1) suggested that the

Table 2 ^{19}F chemical shifts and line widths of 3,7-DF MbCO in 90% $^{1}H_2O$/10% $^{2}H_2O$, pH 7.0, at 25 °C

	$B_0 = 9.4\,T$		$B_0 = 11.7\,T$			$R_{2dia}^{CSA\,a}$ (s^{-1})	
Signal	$\Delta\nu_{1/2}^{obs\,b}$ (*Hz*)	$R_2^{obs\,c}$ (s^{-1})	$\Delta\nu_{1/2}^{obs\,b}$ (*Hz*)	$R_2^{obs\,c}$ (s^{-1})	$\Delta R_2^{obs\,d}$ (s^{-1})	$B_0 = 9.4\,T$	$B_0 = 11.7\,T$
3-F	81 ± 8	254 ± 25	98 ± 10	308 ± 31	54 ± 40	96 ± 72	150 ± 110
7-F	107 ± 11	336 ± 34	129 ± 13	405 ± 41	69 ± 53	122 ± 94	192 ± 150

[a]The contribution of chemical shift anisotropy to transverse relaxation calculated with equation (4) with the assumption of $\omega_I^2\tau_r^2 >> 1$.
[b]Observed line width.
[c]Transverse relaxation rate calculated using $R_2^{obs} = \pi\Delta\nu_{1/2}^{obs}$.
[d]The difference between the transverse relaxation rates at 9.4 T and 11.7 T.

Table 3 ^{19}F chemical shifts and line widths of 3,7-DF deoxyMb in 90% H_2O/10% $^{2}H_2O$, pH 7.0, at 25 °C

	$B_0 = 9.4\,T$		$B_0 = 11.7\,T$					$B_0 = 9.4\,T$	
Signal	$\Delta\nu_{1/2}^{obs\,a}$ (*Hz*)	$R_2^{obs\,b}$ (s^{-1})	$\Delta\nu_{1/2}^{obs\,a}$ (*Hz*)	$R_2^{obs\,b}$ (s^{-1})	$\Delta R_2^{obs\,c}$ (s^{-1})	$\Delta R_{2dia}^{CSA}Z^{d}$ (s^{-1})	$\Delta R_{2para}^{Curie}Z^{e}$ (s^{-1})	$R_{2para}^{Curie\,f}$ (s^{-1})	$\tau_r{}^{g}$ (*ns*)
3-F	710 ± 71	2230 ± 220	910 ± 91	2860 ± 290	630 ± 360	54 ± 40	580 ± 320	1030 ± 570	27 ± 14
7-F	660 ± 66	2070 ± 210	950 ± 95	2980 ± 300	910 ± 370	69 ± 53	840 ± 370	1490 ± 660	39 ± 15

[a]Observed line width.
[b]Transverse relaxation rate calculated using $R_2^{obs} = \pi\Delta\nu_{1/2}^{obs}$.
[c]The difference between the transverse relaxation rates at 9.4 T and 11.7 T. This value arises from the field-dependent properties of both the chemical shift anisotropy (R_{2dia}^{CSA}) and Curie spin relaxation (R_{2para}^{Curie}) contributions.
[d]The difference between the chemical shift anisotropy contributions to the transverse relaxation rate at two magnetic field strengths, obtained from the data for MbCO, and the values are assumed to be equal to ΔR_2^{obs} in Table 2.
[e]The difference between the Curie spin relaxation contributions to the transverse relaxation rate at two magnetic field strengths, obtained by subtraction of the ΔR_2^{CSA} value from the ΔR_2^{obs} one.
[f]The Curie spin relaxation (R_{2para}^{Curie}) contribution calculated from the ΔR_{2para}^{Curie} value.
[g]Correlation time of overall molecular tumbling.

non-equivalence in electronic environment between 3-F and 7-F in the former is larger than that in the latter. These results suggested a difference in electronic nature of 3(or 7)-F–C bond between the two Mb complexes, which in turn influences the R_{2dia}^{CSA} value. Studies on reconstituted Mb possessing appropriate diamagnetic-model heme would be desirable to accurately estimate the R_{2dia}^{CSA} value of deoxyMb. In addition, the precision in the determination of the τ_r value could be also improved by increasing the number of measurements at various field-strengths. On the basis of the estimated τ_r values, it could be at least concluded that 3,7-DF is dynamically fixed to the Mb protein, as has been demonstrated for hemes in various Mbs,[25,26] and hence the present system is in the slow-motion regime, which holds $\omega_I^2\tau_r^2 >> 1$. Finally, in the case of metMb, the field dependence of the line width of the signals was remarkably greater compared with that in the cases of the other Mbs. Extremely large broadening of the signals severely hampered accurate measurement of the $\Delta\nu_{1/2}^{obs}$ values.

With knowledge of the R_{2dia}^{CSA} and R_{2para}^{Curie} values, the line width of the signals as a function of field strength could be estimated (Figure 3b). Owing to the factor $S^2(S+1)^2$ in Equation (14), the R_{2para}^{Curie} value is expected to be larger by factors of 64 and 136 in deoxyMb ($S = 2$) and metMb ($S = 5/2$), respectively, relative to that in $MbCN^-$ ($S = 1/2$), at a given field strength. On the basis of the R_{2para}^{Curie} value of 1490 ± 660 s^{-1} obtained for deoxyMb at 9.4 T, the value for $MbCN^-$ was calculated to be ~23 s^{-1} at the same field strength, which accounts for the line width of ~7 Hz for the signals, confirming that the R_{2para}^{Curie} contribution is negligibly small for the R_{2para} value of the $S = 1/2$ system, as has been described previously.[6] Furthermore, abolition of the higher sensitivity of spectral measurements at higher magnetic field strength caused by the considerable broadening of the signals owing to the increased R_{2para}^{Curie} contribution with increasing field strength was demonstrated for high-spin systems. Hence, spectral measurements of the proteins with large S values, such as deoxyMb and metMb, at higher magnetic field strength cannot make use of the benefits of high sensitivity and resolution, because of the considerable broadening of their signals owing to sharp increases in the R_{2dia}^{CSA} and R_{2para}^{Curie} contributions to spin–spin relaxation rate with increasing field strength (Figure 3b). Consequently, in order to record the spectra of paramagnetic molecules with better sensitivity and resolution, the magnetic field strength used for the measurements needs to be optimized according to their magnetic and dynamic properties.

CONCLUSION

A study on the field dependence of the line width of the NMR signals arising from immobilized fluorine atom(s) introduced to the active site of Mb with various S values has revealed the significant contributions of chemical shift anisotropy and Curie spin to ^{19}F transverse relaxation. Curie spin relaxation dominates paramagnetic ^{19}F transverse relaxation, and the overall correlation time of a protein could be estimated from the results of analysis of Curie spin relaxation.

ACKNOWLEDGEMENTS

We are indebted to Mr Taito Miyazaki for the assistance with recording the ^{19}F NMR spectra. This work was supported by Grants-in-Aid for Scientific Research on Innovative Areas (No. 23108703, 'π-Space', and 23655151) from the Ministry of Education, Culture, Sports, Science and Technology, Japan, the Yazaki Memorial Foundation for Science and Technology, and the NOVARTIS Foundation (Japan) for the Promotion of Science. The NMR spectra were recorded on a Bruker AVANCE-500 spectrometer at the Chemical Analysis Center, University of Tsukuba.

1 Swift, T. J. in *NMR of Paramagnetic Molecules* (eds) La Mar, G. N., Horrocks, Jr. W. D. & Holm, R. H.) Ch. 2, 53–83 (Academic Press, New York, 1973).
2 Yamamoto, Y. NMR Study of Paramagnetic Haemoproteins. *Annu. Rep. NMR Spectrosc.* **36,** 1–77 (1998).
3 Bertini, I., Luchinat, C. & Parigi, G. *Solution NMR of Paramagnetic Molecules* (Elsevier, Amsterdam, 2001).
4 Bertini, I. & Luchinat, C. *NMR of Paramagnetic Molecules in Biological Systems* (The Benjamin/Cummings Publishing Company, Inc., Menlo Park, 1986).
5 Yamamoto, Y., Hirai, Y. & Suzuki, A. ^{19}F NMR study of protein-induced rhombic perturbations on the electronic structure of the active site of myoglobin. *J. Biol. Inorg. Chem.* **5,** 455–462 (2000).
6 Hirai, Y., Yamamoto, Y. & Suzuki, A. ^{19}F NMR study of the heme orientation and electronic structure in a myoglobin reconstituted with a ring-fluorinated heme. *Bull. Chem. Soc. Jpn.* **73,** 2309–2316 (2000).
7 Poliart, C., Briand, J.-F., Tortevoie, F., Leroy, J., Simonneaux, G. & Bondon, A. High sensitivity of the fluorine NMR signals of difluorovinyl analogs of natural hemin: reconstituted heme proteins and self-exchange electron transfer in model compounds. *Magn. Reson. Chem.* **39,** 615–620 (2001).
8 Yamamoto, Y., Nagao, S., Hirai, Y., Inose, T., Terui, N., Mita, H. & Suzuki, A. NMR Investigation of the Heme Electronic Structure in Deoxymyoglobin Possessing a Fluorinated heme. *J. Biol. Inorg. Chem.* **9,** 152–160 (2004).
9 Hirai, Y., Nagao, S., Mita, H., Suzuki, A. & Yamamoto, Y. ^{19}F NMR study on the heme electronic structure in oxy and carbonmonoxy reconstituted myoglobins. *Bull. Chem. Soc. Jpn.* **77,** 1485–1486 (2004).
10 Nagao, S., Hirai, Y., Suzuki, A. & Yamamoto, Y. ^{19}F NMR characterization of the thermodynamics and dynamics of the acid-alkaline transition in a reconstituted sperm whale metmyoglobin. *J. Am. Chem. Soc.* **127,** 4146–4147 (2005).
11 Yamamoto, Y., Nagao, S. & Suzuki, A. ^{19}F NMR Study of *b*-type haemoproteins. *Modern Magn. Reson.* **1,** 531–538 (2006).
12 Sykes, B. & Hull, W. E. Fluorine nuclear magnetic resonance studies of proteins. *Methods Enzymol.* **49,** 270–295 (1978).
13 Gerig, J. T. Fluorine NMR of proteins. *Prog. NMR Spectrosc.* **26,** 293–370 (1994).
14 Abragam, A. *Principles of Nuclear Magnetism* (Oxford University Press, Oxford, 1961).
15 Solomon, I. Relaxation Processes in a System of Two Spins. *Phys. Rev.* **99,** 559–565 (1955).
16 Bloembergen, N. Proton relaxation times in paramagnetic solutions. *J. Chem. Phys.* **27,** 572–573 (1957).
17 Gueron, M. Nuclear relaxation in macromolecules by paramagnetic ions: a novel mechanism. *J. Magn. Reson.* **19,** 58–66 (1975).
18 Vega, A. J. & Fiat, D. Nuclear relaxation processes of paramagnetic complexes. the slow motion case. *Mol. Phys.* **31,** 347–355 (1976).
19 Unger, S. W., Jue, T. & La Mar, G. N. Proton NMR dipolar relaxation by delocalized spin density in low-spin ferric porphyrin complexes. *J. Magn. Reson.* **61,** 448–456 (1985).
20 Yamamoto, Y. Analysis of ^{13}C relaxation of heme peripheral methyl group in ferric low-spin myoglobin. *J. Magn. Reson.* **B103,** 72–76 (1994).
21 Teale, F. W. J. Cleanage of the Haem-protein Link by Acid Methylethylketone. *Biochim. Biophys. Acta* **35,** 543 (1959).
22 Oldfield, E., Norton, R. S. & Alerhand, A. Studies of individual carbon sites of proteins in solution by natural abundance carbon 13 nuclear magnetic resonance spectroscopy: relaxation behavior. *J. Biol. Chem.* **250,** 6368–6380 (1975).
23 Visscher, R. B. & Gurd, F. R. N. Rotational motions in myoglobin assesses by carbon 13 relaxation measurements at two magnetic field strengths. *J. Biol. Chem.* **250,** 2238–2242 (1975).
24 Marshall, A. G., Lee, K. M. & Martin, P. W. Determination of rotational correlation time from perturbed angular correlations of γ rays: apomyoglobin reconstituted with ^{111}Indium(III) mesoprotoporphyrin IX. *J. Am. Chem. Soc.* **102,** 1460–1462 (1980).
25 Johnson, R. D., La Mar, G. N., Smith, K. M., Parish, D. W. & Langry, K. C. Solution deuterium NMR quadrupolar relaxation of heme mobility in myoglobin. *J. Am. Chem. Soc.* **111,** 481–485 (1989).
26 Yamamoto, Y., Inoue, Y., Chujo, R. & Suzuki, T. ^{1}H –NMR study of heme propionate mobility in the active site of myoglobin from *Galeorhinus japonicus*. *Eur. J. Biochem.* **189,** 567–573 (1990).